PHYSICAL REVIEW B VOLUME 40, NUMBER 8 15 SEPTEMBER 1989-I

Second-harmonic generation at simple metal surfaces

A. Liebsch
Institut für Festkörperforschung, Kernforschungsanlage Jülich, D-5170 Jülich, West Germany

W. L. Schaich
Department of Physics, Indiana University, Bloomington, Indiana 47405
(Received 11 April 1989)

The time-dependent density-functional approach is used to determine the frequency dependence of second-harmonic generation (SHG) at various simple metal surfaces. In particular, the function $a(\omega)$ which characterizes the perpendicular surface contribution to the nonlinear polarization is calculated for realistic ground-state density profiles and by taking into account the nonlocal nature of the self-consistent electronic screening response to the applied fields. At the laser frequency of 1.17 eV, the real part of $a(\omega)$ is much larger than the imaginary part and is typically 25–100% larger than in the static limit. Im$a(\omega)$ exhibits a feature for 2ω near the threshold for electron emission and a second one for 2ω near $0.8\omega_p$, where ω_p is the bulk-plasma frequency.

I. INTRODUCTION

Recently, considerable progress has been made in the understanding of the nonlinear electrodynamic response of simple metal surfaces. Weber and Liebsch[1] used the density-functional approach to determine the second-order induced-surface-charge distribution in the low-frequency limit. This treatment incorporates a realistic description of the ground-state electronic density profile as well as the nonlocal nature of the electronic response to an applied electric field. An important discovery of their work is that the nonlinear response of a diffuse profile is significantly larger than that obtained for systems whose profiles have been truncated. This conclusion is drawn by a comparison of their results with the low-frequency limit of the calculations of Corvi and Schaich.[2] The latter authors found the efficiency of second-harmonic generation at arbitrary frequencies, but to do so they used a hydrodynamic model for the electrons' dynamics and represented the surface density profile by a sequence of discrete steps. The cause of the disagreement between the two sets of calculations was clarified by Chizmeshya and Zaremba,[3] who showed that the static density-functional results can be reproduced reasonably well by a generalized Thomas-Fermi model with a realistic density profile. This demonstrates that a semiclassical description of the response to a constant applied field can be in good agreement with a quantum-mechanical theory as long as the electronic density is represented accurately.

These developments raise serious doubts about the *a priori* quantitative accuracy of hydrodynamic estimates at finite frequencies. To address this issue we present here a new calculational scheme which allows the application of a density-functional approach away from the static limit up to a driving frequency of $\omega_p/2$, where ω_p is the bulk-plasma frequency. Part of its formal justification is based on the reanalysis by Schaich and Liebsch[4] of the model treated in Ref. 2. They show that the original numerical results, which were obtained from the full solution of Maxwell's equations, can also be derived from a simpler theory in which certain quantities are calculated in the electrostatic limit. In particular, the intrinsic nonlinear response of electrons in the surface region which is related to the short-range variation of the normal component of the electric field at the metal-vacuum interface, can be calculated by letting the speed of light c be infinite, i.e., by ignoring the long-ranged spatial variation of the transverse electric fields. This simplification is of considerable practical importance since it is then necessary to evaluate only the density response to uniform fields rather than both current and density responses to general fields. The validity of this approximation was demonstrated explicitly in Ref. 4 for the hydrodynamic model. However, it is plausible that the electrostatic limit remains valid more generally since quantum-mechanical corrections to the hydrodynamic model are independent of retardation effects. We use it as the basis of this work.

In agreement with previous authors[5–7] we assume that the second-harmonic–generation amplitude for semi-infinite jellium arises from three contributions: a bulk polarization due to the Lorentz force of the first-harmonic magnetic field acting on the first-harmonic current distribution, a surface polarization parallel to the surface due to the parallel Fresnel electric field acting on the integrated first-harmonic screening charge, and a surface polarization normal to the surface due to nonlocal corrections to the Fresnel fields. Whereas the bulk and parallel surface contributions depend only on macroscopic linear-response properties of the system, the normal surface contribution involves the microscopic nonlinear screening characteristics of the electron gas at the surface. In the notation of Rudnick and Stern,[6] this contribution is represented by the dimensionless function $a(\omega)$ which is proportional to the integrated weight of the normal component of the second-harmonic surface polarization. In the present work, the frequency dependence of $a(\omega)$ is calculated for several simple metal surfaces using a time-dependent (but nonretarded) extension[8,9] of the

density-functional approach.[10] Thus, the ground-state density profile and the nonlocal response to the applied field are calculated self-consistently. In the adiabatic limit, the results for $a(\omega\rightarrow 0)$ coincide with those in Ref. 1 which had been obtained from a purely static density-functional calculation. A preliminary discussion of the frequency dependence of $a(\omega)$ has already appeared.[11]

Since the density-functional approach has led to an excellent understanding of certain linear dynamical response properties (e.g., the local-field enhancement observed in surface photoemission from Al),[12] one has reasons to believe that it might provide an equally successful description of nonlinear dynamical response characteristics. It should be noted, however, that the nonlinear screening involves regions even farther outside in the vacuum tails of the ground-state density profile than does the linear response. For example, in Ref. 1 it was shown that the centroid of the static second-order polarization is located typically 0.5 Bohr atomic units farther from the jellium edge than the static image plane. Since these outer regions of the density are less well described within the local-density approximation, the nonlinear induced dipole moments are presumably somewhat overestimated.[13,14] The second limitation at present is the omission of lattice effects because of our use of the jellium model for the positive ionic charges. Aers and Inglesfield[15] have shown that for Ag(100) much smaller static nonlinear polarizabilities are obtained than for a jellium surface of similar free-electron density. However, as long as the employed laser frequencies are not too close to some interband transition, the time-dependent density-functional scheme in conjunction with the jellium model should be at least qualitatively correct for nearly-free-electron systems and, possibly, for Ag at sufficiently low frequencies. Comparisons of our theoretical predictions of the second-harmonic signal with recent data for Al (Ref. 16) suggest that this is indeed the case.

The outline of this paper is as follows: In Sec. II we present the basic equations for the second-harmonic–generation efficiency in terms of the fundamental quantities that characterize the bulk and surface nonlinear polarizations. We also specify the response equations that determine the linear and nonlinear induced-surface-charge distributions within the time-dependent local-density approximation (TDLDA). Finally, this section contains the derivation of a sum rule which leads to a convenient expression for the nonlinear induced dipole moment. In Sec. III we discuss the results of our calculations, in particular the frequency dependence of $a(\omega)$ for various simple metal surfaces. A summary is given in Sec. IV.

II. THEORY

A. Second-harmonic intensity

Let us assume that linearly polarized light of frequency ω is incident on a semi-infinite jellium system. The polar angle of incidence with respect to the surface normal is denoted as θ and the angle of the polarization vector with respect to the plane of incidence is defined as ϕ ($\phi=0°$ p polarization; $\phi=90°$ s polarization). The generation efficiency of p-polarized second-harmonic reflected output radiation may be parametrized as follows:[2,4]

$$\frac{I_{2\omega}}{I_{\omega}^2}=\frac{8\pi e^2}{m^2\omega^2c^3}\left|\frac{\epsilon(\omega)[\epsilon(\omega)-1]}{\epsilon(\Omega)+s(\Omega)}\times(P\cos^2\phi+S\sin^2\phi)\tan\theta\right|^2, \quad (2.1)$$

where

$$P=\left[a(\omega)\frac{\epsilon(\Omega)}{\epsilon(\omega)}\sin^2\theta-b(\omega)\frac{2s(\omega)s(\Omega)}{\epsilon(\omega)}\cos^2\theta+\frac{d(\omega)}{2}\right][\epsilon(\omega)+s(\omega)]^{-2}, \quad (2.2)$$

$$S=\frac{d(\omega)}{2\epsilon(\omega)[1+s(\omega)]^2} \quad (2.3)$$

with

$$s(\omega)=[\epsilon(\omega)-\sin^2\theta]^{1/2}/\cos\theta\ . \quad (2.4)$$

Here e,m,c are fundamental constants, $\Omega=2\omega$, and $\epsilon(\omega)=1-\omega_p^2/\omega^2$ is the bulk dielectric function with ω_p the bulk-plasma frequency.

The functions $a(\omega)$, $b(\omega)$, and $d(\omega)$ which appear in (2.2) characterize the two nonlinear surface polarizations (normal and parallel to the surface) and the bulk polarization, respectively. As shown by Corvi and Schaich[2] for the hydrodynamic model, this parametrized form of the SHG intensity is nearly identical to the exact radiation obtained from the complete solution of Maxwell's equations. Moreover, these authors found that $b(\omega)$ and $d(\omega)$ are practically independent of frequency and are given by their free-electron values $b(\omega)=-1$ and $d(\omega)=1$. The remaining quantity of interest is the function $a(\omega)$ whose evaluation is the topic of the following subsection. It requires a detailed calculation of the microscopic nonlinear response of electrons in the surface region.

We point out here an interesting feature that does not seem to have been noticed in the past, namely, that the second-harmonic intensity is proportional to the square of the transmission coefficient at the harmonic frequency: $t(2\omega)=2/[\epsilon(2\omega)+s(2\omega)]$. Thus, in contrast to the linear reflectivity, the second-harmonic intensity exhibits a maximum near the minimum of $|\epsilon(2\omega)|$. This behavior, which involves only linear bulk response properties, is apparent in the recent measurements of SHG from Ag,[17] where a pronounced maximum is seen just below $2\omega=3.9$ eV, i.e., below the bulk-plasma frequency. The observed variation of this peak with angle of incidence and with temperature are in qualitative agreement with the behavior expected from the transmission coefficient $t(2\omega)$. Thus, the frequency dependence due to the macroscopic parameters in Eqs. (2.1)–(2.4) can be significant and may outweigh structure due to $a(\omega)$.

B. Density-functional response

As shown in Ref. 4 it suffices to calculate the function $a(\omega)$ in the electrostatic limit, i.e., by considering the density response to a uniform external electric field oriented perpendicular to the surface and varying in time like $e^{-i\omega t}$. The spatial variation of the corresponding applied potential will be taken as $\phi_{\rm app}(z)=-2\pi z$ where z is the coordinate normal to the surface (the jellium background is assumed to occupy the half-space $z\leq 0$). Making use of the translational symmetry parallel to the surface and applying second-order perturbation theory,[18,19] the induced electron distribution near the surface is given by the expression (Hartree atomic units are used unless noted otherwise)

$$\delta n(z,\omega)=\int\frac{d\omega'}{2\pi}\int dz'\,\chi_1(z,z',\omega')\phi_{\rm SCF}(z',\omega')2\pi\delta(\omega-\omega') + \int\frac{d\omega'}{2\pi}\int\frac{d\omega''}{2\pi}\int dz'\int dz''\,\chi_2(z,z',z'',\omega',\omega'')\phi_{\rm SCF}(z',\omega')\phi_{\rm SCF}(z'',\omega'')2\pi\delta(\omega-\omega'-\omega''), \tag{2.5}$$

where χ_1 and χ_2 are the first- and second-order independent-particle susceptibilities of the semi-infinite electron gas. The self-consistent potential $\phi_{\rm SCF}$ differs from the bare applied potential because of local-field effects.

In linear response only that part of δn which oscillates at the frequency ω of the applied field is of interest:

$$\delta n_1(z,\omega)=\int dz'\,\chi_1(z,z',\omega)\phi_{1,\rm SCF}(z',\omega), \tag{2.6}$$

where

$$\phi_{1,\rm SCF}(z,\omega)=\phi_{\rm app}(z)+\delta\phi_1(z,\omega)+\delta V_{1,\rm xc}(z,\omega) \tag{2.7}$$

and $\delta\phi_1$ and $\delta V_{1,\rm xc}$ are the Coulomb and exchange-correlation contributions to the linearly induced potential:[8,9]

$$\delta\phi_1(z,\omega)=-2\pi\int dz'\,|z-z'|\,\delta n_1(z',\omega), \tag{2.8}$$

$$\delta V_{1,\rm xc}=\frac{\partial}{\partial n}V_{\rm xc}(n)\bigg|_{n_0(z)}\delta n_1(z,\omega). \tag{2.9}$$

Here, $V_{\rm xc}$ is the local ground-state exchange-correlation potential and $n_0(z)$ denotes the equilibrium density distribution.

In order to find the nonlinearly induced density that is relevant for second-harmonic generation, we consider those terms in (2.5) which oscillate at frequency $\Omega=2\omega$ and denote them as $\delta n_2(z,\omega)\equiv\delta n(z,\Omega)$. This density obeys the equation

$$\delta n_2(z,\omega)=\int dz'\int dz''\,\chi_2(z,z',z'',\omega,\omega)\phi_{1,\rm SCF}(z',\omega)\phi_{1,\rm SCF}(z'',\omega) + \int dz'\,\chi_1(z,z',\Omega)\{\tfrac{1}{2}V''_{\rm xc}[\delta n_1(z',\omega)]^2+V'_{\rm xc}\delta n_2(z',\omega)+\delta\phi_2(z',\omega)\}, \tag{2.10}$$

where $\delta\phi_2(z,\omega)$ is the Hartree potential corresponding to $\delta n_2(z,\omega)$:

$$\delta\phi_2(z,\omega)=-2\pi\int dz'\,|z-z'|\delta n_2(z',\omega), \tag{2.11}$$

and $V'_{\rm xc}, V''_{\rm xc}$ are the first and second derivatives of $V_{\rm xc}$ with respect to the ground-state density.

The underlying structure of Eqs. (2.6) and (2.10) becomes clearer if we introduce the following "driving" terms or unscreened induced densities:

$$\xi_1(z,\omega)=\int dz'\,\chi_1(z,z',\omega)\phi_{\rm app}(z',\omega), \tag{2.12}$$

$$\xi_2(z,\omega)=\int dz'\int dz''\,\chi_2(z,z',z'',\omega,\omega)\times\phi_{1,\rm SCF}(z',\omega)\phi_{1,\rm SCF}(z'',\omega) + \int dz'\,\chi_1(z,z',\Omega)\tfrac{1}{2}V''_{\rm xc}(\delta n_1(z',\omega))^2. \tag{2.13}$$

We find then that δn_1 and δn_2 obey the same type of self-consistent response equation in which only the driving terms differ ($i=1,2$):

$$\delta n_i(z,\omega)=\xi_i(z,\omega)+\int dz'\,\chi_1(z,z',i\omega)\times\int dz''\,K(z',z'')\delta n_i(z'',\omega). \tag{2.14}$$

Here the function K represents the static linear-response kernel

$$K(z',z'')=-2\pi|z'-z''|+V'_{\rm xc}(n(z'))\delta(z'-z'') \tag{2.15}$$

which accounts for the screening of the "unscreened" induced densities $\xi_1(z,\omega)$ and $\xi_2(z,\omega)$. In principle, the response kernel function K should also be frequency dependent. However, since the TDLDA as described above and the LDA-based random-phase approximation (RPA) (neglect of all terms involving $V'_{\rm xc}$ and $V''_{\rm xc}$ in these

equations while retaining the LDA for the ground state) give qualitatively similar linear and nonlinear induced densities, the static approximation of K is presumably not very severe.[20]

The susceptibility functions χ_1 and χ_2 are given by the expressions[8,9,18,19]

$$\chi_1(z,z',\omega)=\frac{1}{\pi^2}\int_0^{k_F}dk(k_F^2-k^2)\times[\psi_k(z)\psi_k(z')G(z,z',\epsilon_k+\omega)+(\omega\rightarrow-\omega)] \quad (2.16)$$

and

$$\chi_2(z,z',z'',\omega,\omega)=\frac{1}{\pi^2}\int_0^{k_F}dk(k_F^2-k^2)[\psi_k(z)\psi_k(z'')G(z,z',\epsilon_k+2\omega)G(z',z'',\epsilon_k+\omega)+\tfrac{1}{2}\psi_k(z')\psi_k(z'')G(z,z',\epsilon_k+\omega)G(z,z'',\epsilon_k-\omega)+(\omega\rightarrow-\omega)] . \quad (2.17)$$

Here k_F is the Fermi wave vector, ψ_k denotes the bound-state wave functions of the semi-infinite electron system, and G represents the corresponding Green's functions (see definitions in Refs. 21 and 22).

The numerical solution of Eqs. (2.14) is complicated because of the long-range nature of the Coulomb part of the response kernel function K. Rather than using the form given in (2.15) it is more convenient to calculate the Hartree potential from an equivalent expression which contains a short-range kernel:[23]

$$\delta\phi_i(z,\omega)=\int dz'\,e^{-\kappa|z-z'|}\left[\frac{2\pi}{\kappa}\delta n_i(z',\omega)+\frac{\kappa}{2}\delta\phi_i(z',\omega)\right] \quad (2.18)$$

which satisfies the Poisson equation $\delta\phi_i''=-4\pi\delta n_i$ independently of the value of the range parameter κ. In practice, κ is chosen of the order of a Thomas-Fermi screening vector.[22]

As discussed in detail in Ref. 22, the solution of the linear-response equation is simplified further by separating from δn_1 a "model" density δn_{10} which generates the known asymptotic fields in the vacuum and in the interior of the metal. The difference $\delta n_{11}\equiv\delta n_1-\delta n_{10}$ produces only short-range fields which exist in the surface region. The solution of the response equation for δn_{11} can then be obtained by a simple matrix inversion. Since this procedure works well even at very low frequencies we use an analogous method to solve for the second-harmonic density δn_2. In the adiabatic limit the calculated induced densities were found to agree exactly with those in Ref. 1 which were obtained directly by solving the Schrödinger equation in the presence of the uniform static electric field.

To find the self-consistent solution, the model densities are placed at two different positions near the jellium edge and the dipole moment of the resulting induced density of each is calculated. By interpolation we then find that position for which input and output dipole moments coincide. The response equation is then solved once more for this new position in order to verify that the induced density in this case is indeed the self-consistent density.

Finally, the function $a(\omega)$ which characterizes the weight of the perpendicular second-harmonic polarization $P_2(z,\omega)$, is defined by the relation[2,4,6,7]

$$\int_{-\infty}^{\infty}dz\,P_2(z,\omega)\equiv\frac{a(\omega)}{2}\frac{\bar{n}e^3}{2\omega^4m^2}E_{1,\text{in}}^2=\frac{a(\omega)}{4\bar{n}}\left[\frac{E_{1,\text{out}}}{4\pi}\frac{\epsilon(\omega)-1}{\epsilon(\omega)}\right]^2 , \quad (2.19)$$

where $E_{1,\text{out}}$ ($E_{1,\text{in}}$) is the total linear electric field outside (inside) the metal and $\bar{n}>0$ is the bulk density. With our definition of $E_{\text{app}}=2\pi$ we have $E_{1,\text{out}}=2\pi[1+\sigma(\omega)]$ and $E_{1,\text{in}}=2\pi[1-\sigma(\omega)]$ with $\sigma(\omega)$ the integrated first-harmonic induced density

$$\sigma(\omega)=\int_{-\infty}^{\infty}dz\,\delta n_1(z,\omega)=\frac{\epsilon(\omega)-1}{\epsilon(\omega)+1} . \quad (2.20)$$

Then $E_{1,\text{out}}=4\pi\epsilon(\omega)/[\epsilon(\omega)+1]$ and using $(\partial/\partial z)P_2(z,\omega)=\delta n_2(z,\omega)$, we find

$$a(\omega)=-4\bar{n}\int_{-\infty}^{\infty}dz\,z\,\delta n_2(z,\omega)/\sigma(\omega)^2\equiv-4\bar{n}p_2(\omega)/\sigma(\omega)^2 , \quad (2.21)$$

where $p_2(\omega)$ is the dipole moment of the second-harmonic density. Here we have used the fact that the surface second-harmonic polarization vanishes in the interior of the metal, i.e., that the integrated weight of $\delta n_2(z,\omega)$ vanishes.

C. Sum rule for nonlinear induced dipole moment

The calculational route to $a(\omega)$ described above is formally correct but computationally impractical at one step. The direct numerical evaluation of the induced dipole moments,

$$p_i(\omega)=\int_{-\infty}^{\infty}dz\,z\,\delta n_i(z,\omega) , \quad (2.22)$$

is difficult because of the slowly decaying Friedel oscillations that the induced densities exhibit in the interior of the metal. It was shown in Ref. 22 how the dynamical force sum rule[24] can be used in the linear response to circumvent this problem by providing an analytical relation between the full dipole moment and the first moment in the region outside the jellium edge. For a full LDA calculation one has

$$p_1(\omega)=\frac{\epsilon(\omega)-1}{\epsilon(\omega)}\int_0^{\infty}dz\,z\,\delta n_1(z,\omega) . \quad (2.23)$$

Here we derive an analogous sum rule with the second-harmonic density which also relates the full moment to the external moment. Again for the full LDA, it appears as

$$p_2(\omega)=\frac{\epsilon(\Omega)-1}{\epsilon(\Omega)}\left[\int_0^\infty dz\, z\,\delta n_2(z,\omega)+\frac{\sigma(\omega)}{2\bar{n}}\right]. \quad (2.24)$$

The basic argument for the sum rule comes from calculating in two different ways f, the force per unit area on a semi-infinite grounded jellium slab. First, using the total electric field we write

$$f=\int_{-\infty}^\infty dz(-e)n_+(z)E(z)\ , \quad (2.25)$$

where $n_+(z)>0$ describes the variation of the positive background density. For clarity we explicitly show in the rest of this subsection factors of the electron's charge, $e<0$; all the n's in the next several equations are number densities. In the applications of this paper $n_+(z)=\bar{n}\Theta(-z)$ with $\Theta(z)$ the unit step function, but to indicate how the answers change when an adlayer is present we imagine for the derivation that

$$n_+(z)=\bar{n}\Theta(-z)+\delta n_+(z)\ , \quad (2.26)$$

where $\delta n_+(z)$ is nonzero only for $z>0$. Now use Poisson's equation which at the second harmonic has the form $dE_2/dz=4\pi e\delta n_2(z,\omega)$ to reexpress (2.25) and (2.26) as

$$f_2=m\omega_p^2\int_{-\infty}^0 dz\, z\,\delta n_2(z,\omega)$$
$$+m\omega_p^2\int_0^\infty dz\,\delta n_+(z)\int_z^\infty dz'\,\delta n_2(z',\omega)/\bar{n}\ , \quad (2.27)$$

where $\omega_p^2=4\pi e^2\bar{n}/m$. We have assumed here that E_2 vanishes as $|z|\to\infty$.

The alternate way of finding f uses the forces from the applied electric field and the system's electrons to write

$$f=\int_{-\infty}^\infty dz(-e)n_+(z)E_{\rm app}+\sum f_{-+}\ , \quad (2.28)$$

where f_{-+} is the force that a negative charge (an electron) exerts on a positive charge (a piece of the jellium). Adapting the argument of Epstein and Johnson,[25] we note that by action-reaction $f_{-+}=-f_{+-}$ and that f_{+-} appears in the electrons' equation of motion:

$$\frac{\partial}{\partial t}\sum p_-=\sum f_{+-}+\sum f_{--}+\int_{-\infty}^\infty dz\, en(z)E_{\rm app}$$
$$+\int_{-\infty}^\infty dz\, n(z)F_{\rm ext}(z)\ , \quad (2.29)$$

where p_- is an electron momentum, f_{--} is the electron-electron force, and $F_{\rm ext}$ describes the influence of any external potential energy constraining the electrons. This last term is absent in a fully consistent LDA theory but appears when one does an LDA-based RPA calculation or more generally an RPA calculation for a model potential energy such as an infinite or finite step barrier. The potential energy used for the ground-state calculation is for these cases written as

$$V_m(z)=V_{\rm ext}(z)+V_H^0(z)\ , \quad (2.30)$$

where $V_H^0(z)$ is the electronic Hartree potential energy for the ground-state density and $V_{\rm ext}(z)$ varies so $V_m(z)$ represents the model potential energy of the ground state. Then when one does a response calculation, $V_{\rm ext}(z)$ is held fixed while the Hartree term is self-consistently modified by the changes in the electron density.

Now use (2.29) to solve for $\sum f_{-+}$ and substitute in (2.28) to obtain at the second harmonic

$$f_2=\int_{-\infty}^\infty dz\, e\,\delta n_1(z,\omega)E_{\rm app}$$
$$+m\Omega^2\int_{-\infty}^\infty dz\, z\,\delta n_2(z,\omega)$$
$$+\sum f_{--}+\int dz\,\delta n_2(z,\omega)F_{\rm ext}(z)\ , \quad (2.31)$$

where the time derivative of the electrons' momentum has been replaced with a second time derivative of their dipole moment. We further simplify this result by noting that the total force due to electron-electron interactions vanishes and by replacing $\int_{-\infty}^\infty dz\, e\,\delta n_1(z,\omega)$ with $\sigma(\omega)$. Then equating (2.25) and (2.31) yields after some straightforward algebra

$$\int_{-\infty}^\infty dz\, z\,\delta n_2(z,\omega)=\frac{\epsilon(\Omega)-1}{\epsilon(\Omega)}\left[\int_0^\infty dz\, z\,\delta n_2(z,\omega)+\sigma(\omega)\frac{E_{\rm app}}{m\omega_p^2}+\int_{-\infty}^\infty dz\,\delta n_2(z,\omega)\frac{F_{\rm ext}(z)}{m\omega_p^2}\right.$$
$$\left.-\int_0^\infty dz\,\delta n_+(z)\int_z^\infty dz'\,\delta n_2(z',\omega)/\bar{n}\right]. \quad (2.32)$$

If we ignore $F_{\rm ext}$ and δn_+ and replace $E_{\rm app}$ with 2π as we revert to atomic units, then (2.32) becomes (2.24). If we further go to the static limit, the result reduces to that of Budd and Vannimenus.[26] For a LDA-based RPA calculation $F_{\rm ext}=-(\partial/\partial z)V_{\rm xc}$ so with δn_+ set to zero the generalization of (2.24) is

$$p_2(\omega)=\frac{\epsilon(\Omega)-1}{\epsilon(\Omega)}\left[\int_0^\infty dz\, z\,\delta n_2(z,\omega)+\frac{\sigma(\omega)}{2\bar{n}}-\omega_p^{-2}\int_{-\infty}^\infty dz\,\delta n_2(z,\omega)\frac{\partial}{\partial z}V_{\rm xc}\right]. \quad (2.33)$$

At the same level (2.23) should be generalized to[22]

$$p_1(\omega)=\frac{\epsilon(\omega)-1}{\epsilon(\omega)}\left[\int_0^\infty dz\, z\,\delta n_1(z,\omega)-\omega_p^{-2}\int_{-\infty}^\infty dz\,\delta n_1(z,\omega)\frac{\partial}{\partial z}V_{\rm xc}\right]. \quad (2.34)$$

III. RESULTS AND DISCUSSION

Figure 1 shows the real and imaginary parts of the second-harmonic density $\delta n_2(z,\omega)$ for $r_s=3$ at several frequencies below $0.5\omega_p$. The integrated weight of these induced densities vanishes. Thus, at low frequencies, the main feature near the jellium edge has dipolar shape with weak Friedel oscillations extending into the interior. Towards higher frequencies, however, the oscillations become very prominent so that it is no longer justified to speak of a main peak localized within a Thomas-Fermi screening length of the surface. Instead, the range over which the second-harmonic density is large, extends several tens of angstroms into the metal.

In the adiabatic limit, the period of the Friedel oscillation is $2k_F$ as in the case of the linear induced density. At small but finite frequencies, the wave vector of this oscillation increases according to the relation $q/k_F=1+(1+2\omega/E_F)^{1/2}$. At higher frequencies ($\omega\gtrsim 0.3\omega_p$) a new, long-wavelength oscillation becomes important whose wave vector obeys roughly the relation $q/k_F=\omega/E_F$. The actual wave vectors of these oscillations at the fundamental frequencies $\omega=0.3\omega_p$ and $0.4\omega_p$ are plotted in Fig. 2 for various bulk densities. This graph shows that the long-wavelength Friedel oscillation are in fact better described by the so-called emission threshold wave vectors[27] $q/k_F=(V/E_F)^{1/2}-[(V-2\omega)/E_F]^{1/2}$ (see thin solid lines in Fig. 2) where V is the height of the surface-barrier potential and E_F is the Fermi energy. In the linear case, the dominant short- and long-wavelength wave vectors were found to be given by $q/k_F=1+(1+\omega/E_F)^{1/2}$ and $q/k_F=(V/E_F)^{1/2}-[(V-\omega)/E_F]^{1/2}$ (for $V-E_F<\omega<V$), respectively.[22,27] Thus, the oscillations exhibited by the harmonic induced density in the entire frequency range below $0.5\omega_p$ seem to be dominated by the linear screening at 2ω as indicated by the second term in Eq. (2.14) involving $\chi_1(z,z',2\omega)$. The same behavior was observed for all other bulk densities ($r_s=2,3,4,5$).

The large penetration depth of the harmonic density seen for $\omega\gtrsim 0.3\omega_p$ was also obtained for other bulk densities. These results have important consequences for SHG from thick alkali overlayers (10–50 Å).[28,29] For example, in the case of Rb ($r_s=5.25$), the laser frequency of

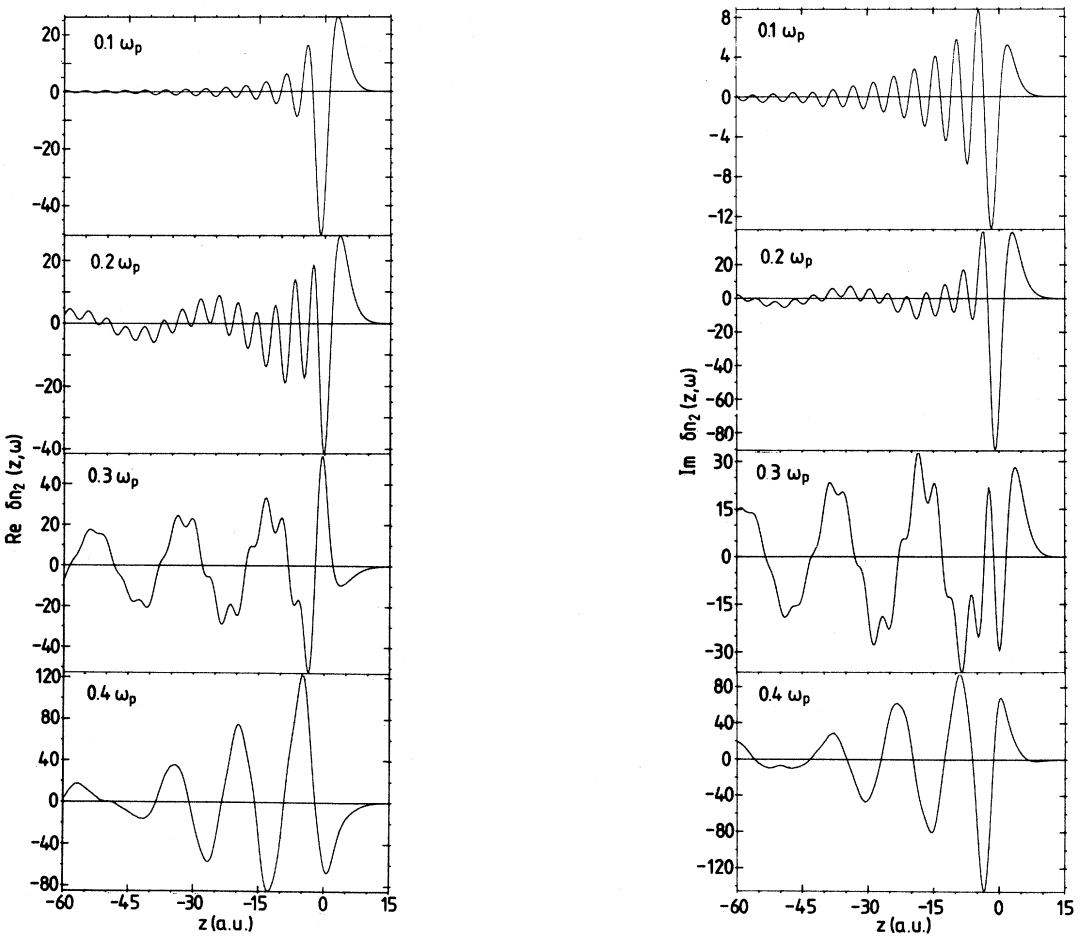

FIG. 1. Second-harmonic induced screening density for $r_s=3$ at several frequencies below $0.5\omega_p$ where ω_p is the bulk-plasma frequency. The positive background occupies the half-space $z\leq 0$.

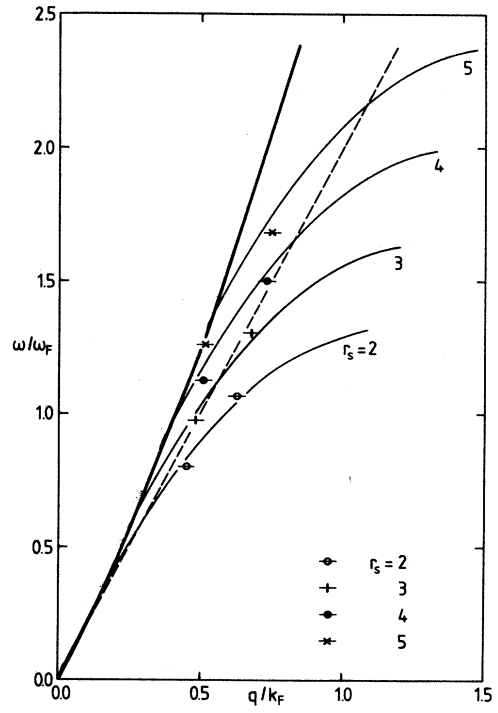

FIG. 2. Wave vectors of second-harmonic induced densities for various bulk densities at frequencies $0.3\omega_p$ (lower symbol) and $0.4\omega_p$ (upper symbol). The width of the bars indicates the uncertainty of determining the wavelengths from the graphs of $\delta n_2(z,\omega)$. Thin solid lines denote threshold oscillations (see text); dashed line denotes $q/k_F=0.5\omega/E_F$; heavy solid line denotes left boundary of bulk electron-hole pair excitation spectrum, $q/k_F=(\omega/E_F+1)^{1/2}-1$.

1064 nm $=1.17$ eV corresponds to about $0.3\omega_p$. At this frequency, therefore, the second-harmonic signal cannot be considered as originating separately at the vacuum-adsorbate and adsorbate-substrate interfaces. Instead, the perpendicular surface polarization extends across the entire overlayer and involves electrons at both interfaces. It would be interesting to investigate whether these slowly decaying Friedel oscillations can lead to standing waves between the two interfaces.

According to the relations (2.21) and (2.24), the function $a(\omega)$ which specifies the weight of the normal surface polarization, is given by the first moment of the harmonic densities shown in Fig. 1. The frequency dependence of the real and imaginary parts of $a(\omega)$ is plotted in Fig. 3 for various bulk densities. The imaginary part clearly exhibits two features: a maximum near $\omega=\Phi/2$ where Φ is the work function and a second maximum near $\omega=0.4\omega_p$. For large r_s these features cannot be resolved since $\Phi/2$ is too close to $0.4\omega_p$. The real part of $a(\omega)$, which agrees for $\omega\to 0$ with the previously calculated static values,[1] shows the typical behavior expected from Kramers-Kronig relations. The results shown in Fig. 3 correspond to the full TDLDA. They improve earlier, more approximate results[11] which were derived for a simplified linear self-consistent potential in the nonlinear driving term and which erroneously used ω rather than Ω in the frequency argument of the linear susceptibility χ_1 in the second term of (2.10).

The spectral features that we find for $\mathrm{Im}a(\omega)$ can be directly correlated with similar features exhibited by $\mathrm{Im}d_\perp(\omega)$, the imaginary part of the centroid of the linearly induced screening density, $d_\perp(\omega)\equiv p_1(\omega)/\sigma(\omega)$. As discussed in detail in Refs. 22, 27, and 30, $\mathrm{Im}d_\perp(\omega)$, which is a measure of the power absorption due to excitation of electron-hole pairs in the surface region, increases at first linearly with ω, then more rapidly when ω passes through the threshold for electron emission, and finally near $0.8\omega_p$ shows the well-known resonance[31] that is also observed in surface photoemission.[12] Similarly, $\mathrm{Im}a(\omega)$ first rises significantly when 2ω is near threshold, even developing a separate peak if the bulk density is large enough, and then shows a resonance structure near $2\omega\approx 0.8\omega_p$. This resonance in the nonlinear response is always present but becomes more prominent towards larger r_s values, where the surface barrier is smoother. The same trend is found in the linear case.

One of the important results of the nonlinear density-functional–response calculations is the overall magnitude of the parameter $a(\omega)$. In Table I we list the static values of $a(\omega)$ for various bulk densities and for different kinds of response treatments. This comparison demonstrates the extreme sensitivity of $a(\omega=0)$ to the details of the ground-state density profile. Model densities such as those obtained for the infinite potential barrier are not sufficiently polarizable and give accordingly too small values of $a(0)$. Surprisingly, even the finite-barrier model, which gives much smoother density profiles than the infinite-barrier model, leads also to serious underestimates of $a(0)$.

To illustrate this point further, we show in Fig. 4 the value of $a(0)$ for a series of model potentials of the form $V(z)=V/(e^{\alpha z}+1)$ where V is the height of the surface-barrier potential obtained within the LDA for a given bulk density. For $\alpha=0.5$ a.u., $a(0)$ nearly coincides with the corresponding LDA value. As α increases, the surface potential as well as the electron distribution become stiffer and the polarizability diminishes. In the limit of large α, $a(0)$ approaches the value obtained for the finite-barrier model (single-step surface potential; see Table I).

On the other hand, it is known that the local approximation to the exchange-correlation functional is less applicable at low densities. As a consequence, the polarizability of the tail region of the density is presumably overestimated in the LDA. One indication of this effect is the $\approx 25\%$ reduction of $|a(0)|$ that we obtain if exchange-correlation contributions to the induced potential are omitted, i.e., if the response to the external perturbation is treated within the RPA (see Table I). It would be of interest to determine the magnitude of $a(\omega=0)$ within a nonlocal exchange-correlation scheme.

In order to check the importance of exchange-correlation effects for the frequency dependence of $a(\omega)$, we have also carried out RPA-type response calculations at finite ω (the ground-state properties are described

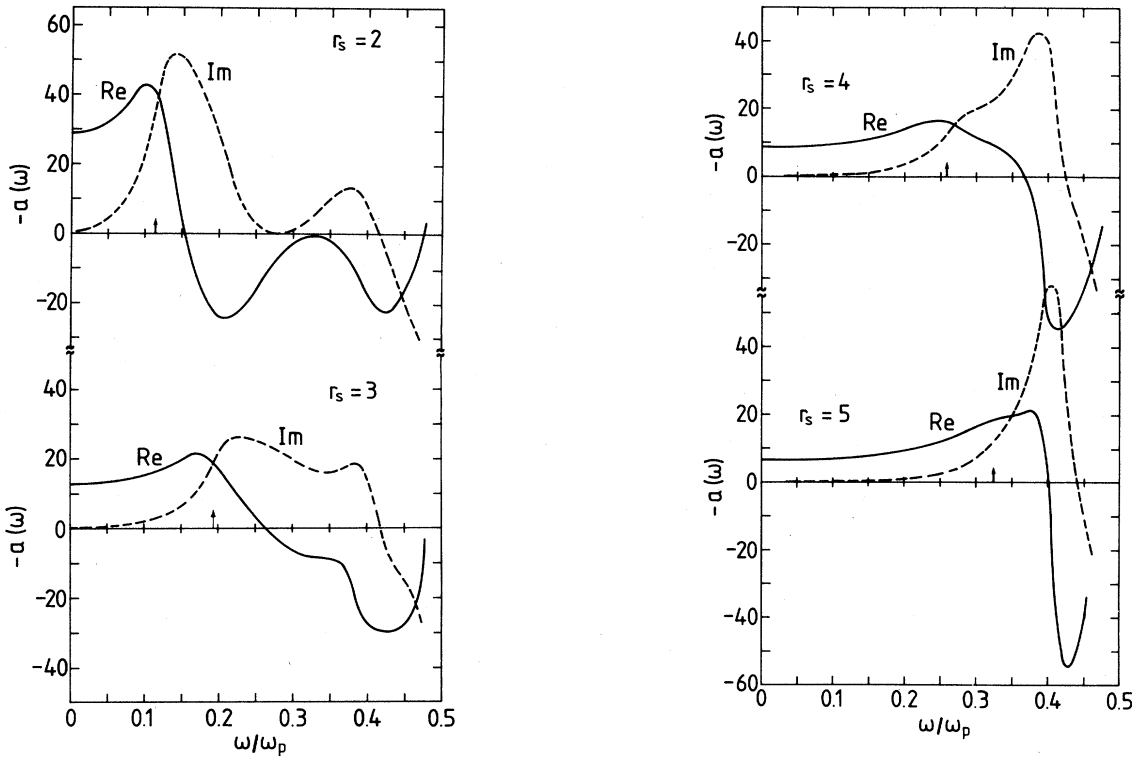

FIG. 3. Frequency dependence of $a(\omega)$ for various r_s calculated within the time-dependent density-functional approach. The vertical arrows denote $\Phi/2$ where Φ is the work function.

within the LDA). These results are shown in Fig. 5. The qualitative behavior of $a(\omega)$ is similar to that in the consistent LDA approach. The overall magnitude is somewhat reduced and the resonance near $0.4\omega_p$ is shifted to slightly higher frequencies. These modifications are analogous to those which have been found previously for linear response.[22,27,30] The relatively small difference between RPA and LDA suggests that improved descriptions of electron-electron interactions at finite frequencies will not lead to a significantly different frequency dependence of $a(\omega)$.

At the laser frequency of 1.17 eV, the real part of $a(\omega)$ is typically 25% (for $r_s=2$) to 100% (for $r_s=5$) larger than in the static limit, while the imaginary part of $a(\omega)$

TABLE I. Adiabatic values $-a(\omega=0)$ for various bulk densities and surface response treatments: LDA (Ref. 1); LDA-RPA (ground state: LDA, response to static field in RPA); FBM-RPA (finite-step potential barrier, step height from LDA, response in RPA); IBM-RPA (infinite-step potential barrier, response in RPA); one-step (single-step ground-state density, hydrodynamic response, from Ref. 2); ext-Th-F (extended Thomas-Fermi calculation, from Ref. 3).

	r_s			
	2	3	4	5
LDA	28.4	12.9	8.6	6.6
LDA-RPA	22.1	10.0	6.6	5.0
FBM-RPA	7.0	4.0	3.2	2.8
IBM-RPA	0.8	1.0	1.2	1.5
One-step	$\frac{2}{9}$	$\frac{2}{9}$	$\frac{2}{9}$	$\frac{2}{9}$
Ext-Th-F	34.7	14.9	8.9	6.2

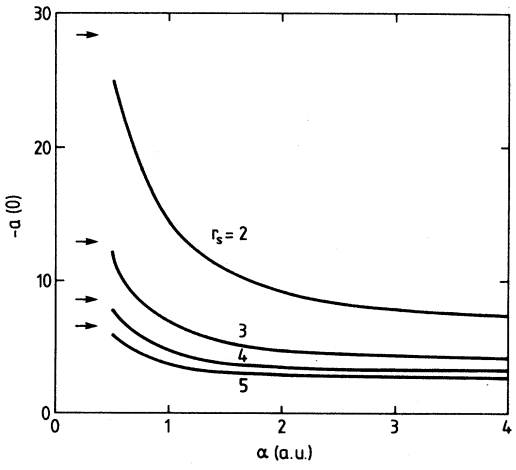

FIG. 4. Variation of $a(0)$ for increasingly stiffer surface potential of the form $V(z)=V/(e^{\alpha z}+1)$ where V is the surface-barrier height calculated within the LDA. The arrows mark the LDA values of $a(0)$ (see Table I).

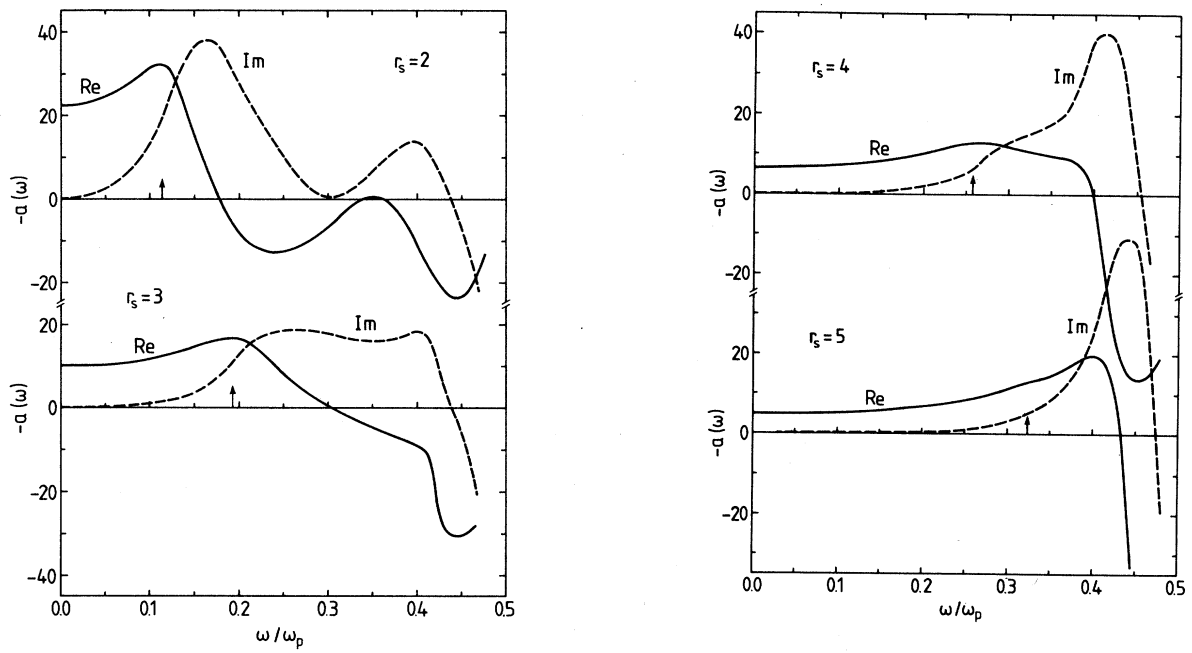

FIG. 5. Frequency dependence of $a(\omega)$ for various r_s calculated within the LDA-based RPA. The vertical arrows denote $\Phi/2$ where Φ is the work function.

is still rather small [20–30 % of Re$a(\omega)$]. The adiabatic values can therefore be considered as representative of the low-frequency behavior of $a(\omega)$. Accordingly, we can expect in this range a similar dependency of $a(\omega)$ on surface conditions as in the static limit. Thus, if the surface electrons of the semi-infinite free-electron system would take part in more localized chemisorption bonds, their polarizability would be reduced and the magnitude of $a(\omega)$ would diminish.

IV. SUMMARY

For simple metals, it has been known for a long time that second-harmonic generation originates from a bulklike magnetic dipole source polarization and two surface polarizations related to the rapid variation of the normal component of the electric field in the vicinity of the surface. Of these three sources, the bulk and parallel surface contributions are not surface sensitive as they depend only on bulk macroscopic screening properties at the fundamental and harmonic frequencies. The perpendicular surface harmonic polarization, however, is determined by the nonlinear dynamic response of the surface electrons. It is this term which is primarily responsible for the surface sensitivity of SHG. Since this contribution depends sensitively on the details of the electron distribution at the surface, it is necessary to calculate it quantum mechanically and to account for the self-consistent screening of the surface charges that are induced by the external electromagnetic fields.

In the present work we have used the time-dependent density-functional approach to calculate the frequency dependence of the function $a(\omega)$ which characterizes the perpendicular SH surface polarization. Since we are primarily concerned with the nonlinear response of conduction electrons at simple metal surfaces, the positive ionic charges are treated within the jellium model. For all bulk densities that we have studied, we have found that $a(\omega)$ exhibits two characteristic features, one related to the threshold for emission ($2\omega\approx$ work function) and another related to the electron-hole–pair resonance or quasicollective mode ($2\omega\approx 0.8\omega_p$). These features are analogous to those familiar from the frequency dependence of the linear surface response function $d_\perp(\omega)$. As a result of these spectral features, both real and imaginary parts of $a(\omega)$ vary appreciably with ω and also change their sign. Obviously, these effects have important consequences for the angle of incidence and polarization dependence of the SH intensity.

At low frequencies, the imaginary part of $a(\omega)$ is relatively small and the real part is somewhat larger than in the adiabatic limit. As we have shown in a previous work,[11] the magnitude and sign of $a(\omega)$ in this region lead to characteristic features which should be observable experimentally. Recent data by Murphy *et al.*[16] indicate that these predictions agree rather well with SHG from clean Al surfaces at the fundamental frequency of 1.17 eV. Earlier data on Al and Ag,[5,32,33] which were analyzed with $a(\omega)$ of the order of unity, were presumably influenced by surface conditions. As we have argued above, adsorbates on such surfaces will tend to reduce the nonlinear polarizability of the surface-electronic density and thereby reduce the overall magnitude of $a(\omega)$. The perpendicular SH surface polarization in this case tends to be dominated by the bulk magnetic dipole and the parallel surface contributions.

ACKNOWLEDGMENTS

This collaboration was supported in part by the North Atlantic Treaty Organization through Grant No. 089/87. The work of W.L.S. was also supported in part by the National Science Foundation through Grant No. DMR-85-12709.

[1]M. Weber and A. Liebsch, Phys. Rev. B **35**, 4711 (1987); **36**, 6411 (1987); **37**, 1019(E) (1988).
[2]M. Corvi and W. L. Schaich, Phys. Rev. B **33**, 3688 (1986).
[3]A. Chizmeshya and E. Zaremba, Phys. Rev. B **37**, 2805 (1988).
[4]W. L. Schaich and A. Liebsch, Phys. Rev. B **37**, 6187 (1988).
[5]N. Bloembergen, R. K. Chang, S. S. Jha, and C. H. Lee, Phys. Rev. **174**, 813 (1968).
[6]J. Rudnick and E. A. Stern, Phys. Rev. B **4**, 4272 (1971).
[7]J. E. Sipe and G. I. Stegeman, in *Surface Polaritons,* edited by V. M. Agranovich and D. L. Mills (North-Holland, New York, 1982), p. 661.
[8]A. Zangwill and P. Soven, Phys. Rev. A **21**, 1561 (1980).
[9]M. J. Stott and E. Zaremba, Phys. Rev. A **21**, 12 (1980).
[10]P. Hohenberg and W. Kohn, Phys. Rev. **136**, B864 (1964).
[11]A. Liebsch, Phys. Rev. Lett. **61**, 1233 (1988); **61**, 1897(E) (1988).
[12]H. Levinson, E. W. Plummer, and P. J. Feibelman, Phys. Rev. Lett. **43**, 952 (1979).
[13]K. R. Subbaswamy and G. D. Mahan, J. Chem. Phys. **84**, 3317 (1986).
[14]G. Senatore and K. R. Subbaswamy, Phys. Rev. A **34**, 3619 (1986).
[15]G. C. Aers and J. E. Inglesfield, J. Phys. C (to be published).
[16]R. Murphy, M. Yeganeh, and E. W. Plummer, Bull. Am. Phys. Soc. **34**, 837 (1989); R. Murphy, M. Yeganeh, K. J. Song, and E. W. Plummer, Phys. Rev. Lett. **63**, 318 (1989).
[17]J. M. Hicks, L. E. Urbach, E. W. Plummer, and H. L. Dai, Phys. Rev. Lett. **61**, 2588 (1988).
[18]A. Zangwill, J. Chem. Phys. **78**, 5926 (1983).
[19]G. Senatore and K. R. Subbaswamy, Phys. Rev. A **35**, 2440 (1987).
[20]E. K. U. Gross and W. Kohn, Phys. Rev. Lett. **55**, 2850 (1985).
[21]A. Liebsch, J. Phys. C **19**, 5025 (1986).
[22]A. Liebsch, Phys. Rev. B **36**, 7378 (1987).
[23]M. Manninen, R. Nieminen, P. Hautojärvi, and J. Arponen, Phys. Rev. B **12**, 4012 (1975).
[24]R. S. Sorbello, Solid State Commun. **48**, 989 (1983); **56**, 821 (1985).
[25]S. T. Epstein and R. E. Johnson, J. Chem. Phys. **51**, 188 (1969).
[26]H. F. Budd and J. Vannimenus, Phys. Rev. B **12**, 509 (1975).
[27]K. Kempa and W. L. Schaich, Phys. Rev. B **37**, 6711 (1988).
[28]H. W. K. Tom, C. M. Mate, X. D. Zhu, J. E. Crowell, Y. R. Shen, and G. A. Somorjai, Surf. Sci. **172**, 466 (1986).
[29]K. J. Song, D. Heskett, H. L. Dai, A. Liebsch, and E. W. Plummer, Phys. Rev. Lett. **61**, 1380 (1988).
[30]K. Kempa, A. Liebsch, and W. L. Schaich, Phys. Rev. B **38**, 12 645 (1988).
[31]P. J. Feibelman, Progr. Surf. Sci. **12**, 287 (1982).
[32]H. Sonnenberg and H. Heffner, J. Opt. Soc. Am. **58**, 209 (1968).
[33]J. C. Quail and H. J. Simon, Phys. Rev. B **31**, 4900 (1985).